A METHODOLOGY FOR CHARACTERIZING REPRESENTATIVENESS IN POWER PLANT PERFORMANCE INDICATOR MEASUREMENTS WITH CFD SIMULATIONS

U. Otgonbaatar, E. Baglietto and N. Todreas
Department of Nuclear Science and Engineering, Massachusetts Institute of Technology,
77 Massachusetts Avenue, Cambridge, MA 02139, USA
uugan_88@mit.edu

ABSTRACT

The measurement of the Steam Generator feedwater mass flow rate is a dominant source of uncertainty in nominal thermal power calculation of a plant. In this paper, mass flow rate measurement by means of an orifice plate is considered. RANS simulation was performed using the CFD code STAR-CCM+ to quantify the representativeness uncertainty of mass flow rate measured in a dedicated experimental configuration. The representativeness uncertainty arises from applying the tolerance values prescribed by the standard in non-straight piping geometries. The simulation results were compared with the test results and the uncertainty bounds prescribed by the ISO standard, demonstrating the feasibility of applying RANS in an industrial setting for a sub 1% uncertainty application. RANS results were also used to identify a variability of measurement result with respect to angular location of pressure tap used in the flow rate measurement. Secondly, a LES was performed on a straight piping configuration to simulate the unsteady coherent flow shedding at the orifice plate. The spectral results of LES were compared with data from a test. The time-averaged LES results are within 0.1% of the value prescribed by the ISO standard. Direct comparison of temporal spectrum of the LES result to the test data is not possible due to the measurement technique. This work is a part of a wider effort to develop a methodology to characterize, assess, and quantify representativeness uncertainty in performance indicator measurements of plants. Spatial, temporal and modeling representativeness uncertainties are presented in this current work.

KEYWORDS: flow rate measurement, orifice plate, Large Eddy Simulation, turbulence, representativeness uncertainty, methodology

1 INTRODUCTION

The uncertainty in thermal power calculation affects the power level at which the plant is allowed to operate. Reducing the uncertainty allows the plant operator to increase the rated power without compromising reliability and safety. An increase in power output translates into increased revenue stream and improved economic competitiveness for the plant. Therefore, it is of great interest to reduce uncertainty in the thermal power calculation.

The Steam Generator (SG) feedwater mass flow rate is the largest source of uncertainty in the calculation of nominal thermal power in pressurized water reactors. In France, the uncertainty in SG feedwater flow measurement represents 80% of the total uncertainty in the thermal power calculation [1].

Mass flow rate measurement by means of an orifice plate is a commonly employed method used in 70% of all flow rate measurements in France. In this method, flow is restricted by an orifice of smaller diameter, internal to the conduit, creating a pressure differential upstream and downstream of the orifice. Mass flow rate is then calculated from the pressure drop as prescribed in ISO-5167 standard [2].

In this paper, results are presented for both Reynolds Averaged Navier Stokes (RANS) and Large Eddy Simulations (LES) performed using the CFD code STAR-CCM+ to simulate the mass flow measurement process using an orifice plate. The overarching aim of the CFD simulations in this work is to study the feasibility of using CFD to reduce uncertainty in a real industrial configuration of mass flow measurement. The possibility of achieving an accuracy of less than 1.0% with RANS models applied to an industrial application is investigated, and the dominant sources of modeling uncertainties are assessed.

The results presented in this paper are part of a larger Ph.D project on developing methodology to identify, assess and reduce uncertainty due to representativeness[3] in performance indicators of nuclear power plants. Representativeness uncertainty arises due to the inherent spatial or temporal variations of the quantity intended to be measured or inadequacy of model. It is the difference between true value of the desired quantity and measured quantity value (adopted from the definition of aleatory uncertainty given by Oberkampf et al [3]). Spatial representativeness uncertainty associated with mass flow rate measurement by an orifice plate presented in this paper is the first of several case studies on which the methodology will be based.

2 FLOW RATE MEASUREMENT BY AN ORIFICE PLATE

The conventional method, currently in practice, for mass flow rate measurement by means of an orifice plate is prescribed by ISO-5167[2]. Figure 1 shows a simple schematic of an orifice plate used for flow rate measurement. Mass flow rate is then calculated from the measured pressure difference as given in Equation (1):

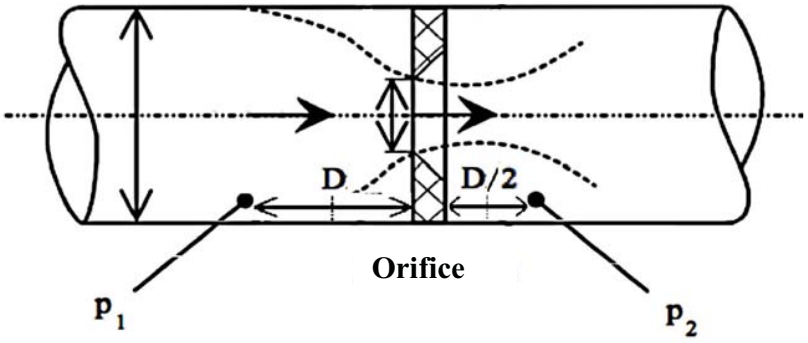

Figure 1: Schematic of flow rate measurement by orifice plate

$$q_m = \frac{\pi}{4} C \frac{1}{\sqrt{1-\beta^4}} d^2 \sqrt{2(p_1 - p_2)\rho} \tag{1}$$

where q_m is the mass flow rate, d is the orifice diameter, D is conduit diameter, p_1 and p_2 are upstream and downstream pressure values, ρ is the density of the fluid and $\beta = d/D$. C is the discharge coefficient prescribed by the standard for given pressure tap configurations.

According to the ISO-5167 standard, the upstream length between the orifice plate and first non-straight pipe section must be greater than a prescribed length or else an additional uncertainty is imposed. For the specific pipe geometry considered in this paper, the ISO-5167 standard requires 28D for a guaranteed accuracy of ± 0.7% or additional uncertainty of 0.5% is imposed [1]. We performed CFD simulations with the aim to assess the deviation from ISO value when upstream piping length is shorter than the minimum required length by the standard.

First, Reynolds Averaged Navier Stokes (RANS) simulations were performed using the CFD code STAR-CCM+ in order to determine the extent of uncertainty in mass flow measurement when the upstream distance from the orifice to the first non-straight section is shorter than the value required by the standard. The geometry chosen for the simulation is a test loop at a facility in France. The simulation results were compared with the test results, as well as the ISO standard. The performance of RANS simulations adopting the standard k-ε and an optimized non-linear k-ε turbulence model [4] are assessed first.

Second, LES was performed in order to capture the physical process of unsteady coherent flow shedding past the orifice edge. The LES runs were performed on a straight pipe geometry representing a field test at a plant. The time-averaged results of LES were benchmarked with the ISO standard, and time spectra of the pressure drop produced by LES are compared with the field test data.

3 TEST/EXPERIMENTAL DATA ON MASS FLOW MEAUSUREMENT BY ORIFICE PLATE

Two different sets of experimental/test data were used to benchmark RANS and LES simulations. Both data sets were obtained in a controlled environment with the objective of quantifying the extent of uncertainty in mass flow rate measurement using an orifice plate.

3.1 Experimental Results of mass flow measurement with non-straight inlet and outlet geometry

The experimental test was conducted at the EDF's EVEREST facility in Chatou, France in order to assess the uncertainty related to the adoption of standards in calculations involving orifice plates for flow rate measurement, for the particular condition of reduced upstream flow development. The experimental test pipe diameter is D=252mm, and the orifice inner diameter is d=173mm with a $\beta = 0.686$.

The experimental piping geometry is given in Figure 2 where inlet T-junction and outlet elbows are indicated in pink and orange along with the location of the orifice plate. The orifice plate is located at 28D distance downstream the inlet T-junction. Upstream and downstream piping geometries do not allow sufficient length for the flow to fully develop leading to a spatial representativeness issue when adopting the ISO standard.

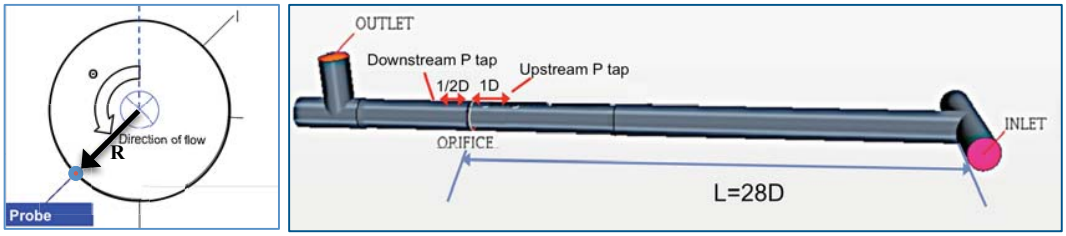

Figure 2: Angular location of pressure taps (left) and geometry of the experimental test (right)

Cylindrical coordinates were used with z axis along the direction of fluid in the straight section of the geometry (shown on the left in Figure 2) in order to understand the heterogeneity of pressure field due to lack of fully developed flow.

During the experiment, two pressure taps are used to measure the pressure drop across the orifice plate. The upstream pressure tap is located at distance D and downstream tap is at distance D/2 as given in right Figure 2. The angular location of the probes are at 135° from the vertical axis as given in left Figure 2.

A controlled flow rate was induced through an orifice plate, and the pressure difference between upstream and downstream pressure values was measured. The values of reference flow rate and flow rate calculated using the orifice plate methods are compared. Flow rate was controlled to 5 different reference values, and pressure drop through the orifice plate was measured. Mass flow rate was then reconstructed using the pressure drop and standard method outlined in section 2.

The results of the experiment on the test geometry are given in **Figure 3** [5] showing the deviation of mass flow rates calculated by the orifice plate method from the reference value as a percentage. The error bars in the experimental result arises from uncertainties in measurement of physical properties of the fluid such as temperature, density; geometrical dimensions of the loop such as d, and D; and the ISO tolerance levels given by the standard.

The systematic shift between the experimental results and the ISO standard is to be expected since the test geometry of the experiment does not respect the upstream flow development length before the first non-straight section of the pipe. In other words, the systematic shift of about 0.5% shown in **Figure 3** is the systematic uncertainty due to non-straight upstream piping geometry as identified by experiment.

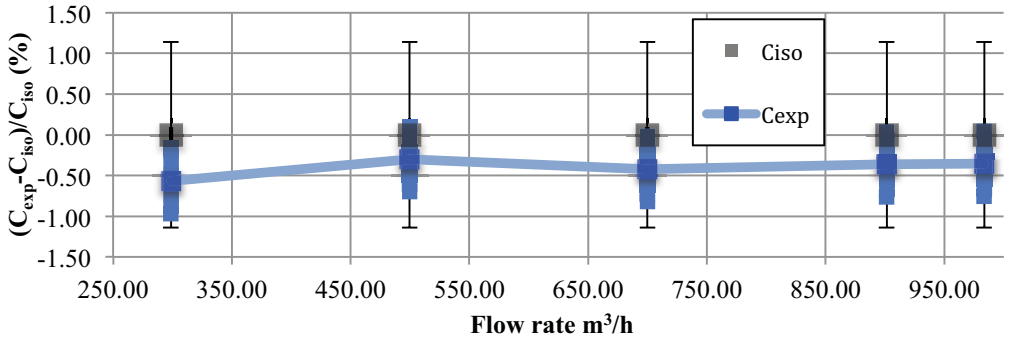

Figure 3: Experimental result expressed in terms of discharge coefficient along with ISO. Error bars of both the standard and experiment are shown.

3.2 Test Data on time dependent pressure drop across an orifice plate

High frequency test measurements (1000Hz) on pressure drop across an orifice plate used to measure a mass flow rate were obtained at an operating plant in France. The purpose of the test was to understand the fluctuation of the differential pressure signal used to calculate feedwater mass flow rate to Steam Generator. Three sets of available data at 100%, 80%, 50% power level flow rates are shown in Figure 4 illustrating that enhanced high frequency noise appears at the 100% power level.

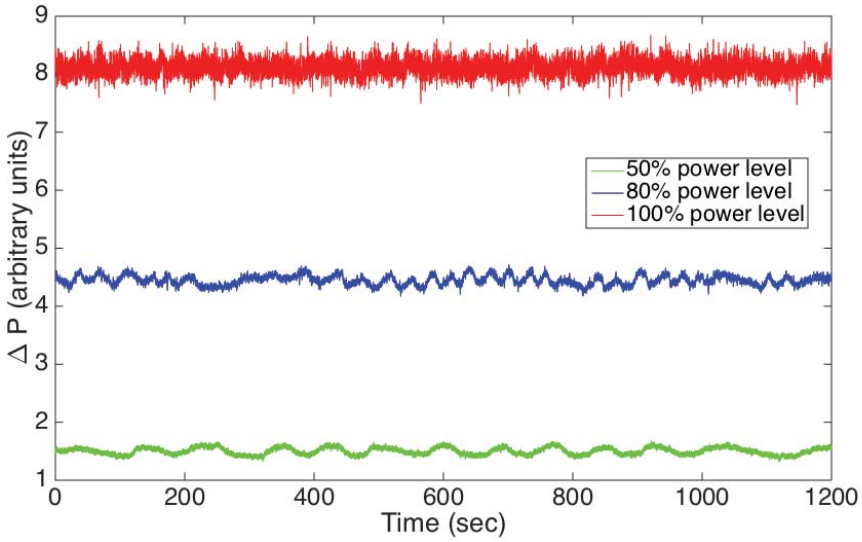

Figure 4: Test data of pressure drop across an orifice plate at flow rates corresponding to 100, 80, 50% power levels

4 CFD SIMULATIONS

In this section, implementation and results of both RANS and LES are discussed. In section 4.1, details on the setup of RANS is discussed, followed by benchmarking results and application to the geometry in question. In section 4.2, mesh generation, boundary conditions, and the results of LES performed on the industrial test geometry are first discussed. Next, benchmark of LES results with the ISO standard, and comparison of spectral analysis using the simulation results are given.

4.1 RANS Simulation to identify Spatial Representativeness Uncertainty

This section focuses on CFD simulation effort on an experimental test configuration of an orifice plate at the test facility described in section 3.1.

The simulation effort in this section is aimed at replicating the experimental flow conditions by including the precise geometrical shape of the upstream and downstream piping and orifice edge shape. Then the simulation results were benchmarked with the experiment and the standard, and sources of uncertainty and the quantities affecting the CFD model are identified.

4.1.1 RANS simulation

Steady state RANS simulations have been performed on a computational domain that replicates the complete 3-dimensional experimental piping layout shown in Figure 2.

Two variants of the k-ε turbulence model are adopted in combination with standard wall function approach, necessary to limit the cell count, given the very high Reynolds number of the experiment. A segregated flow solver based on the SIMPLE algorithm applied on collocated variables with Rhie-Chow interpolation is used. All convective terms are approximated with a non-oscillatory 2nd order scheme using the Venkatakrishnan reconstruction gradient limiting.

An unstructured computational mesh was generated using the STAR-CCM+ built in meshing algorithms, in particular the Trim and prism layer meshers were adopted, which allow producing hexa dominant cells, in combination with boundary fitted cells in the near wall region. The base size of cells is 5mm, and two prism layers with absolute thickness of 1mm and stretching factor 1.5 were used. Volumetric mesh refinement in the region near orifice of 25% of the base size was employed to better resolve the region of important turbulent shedding. This resulted in a total of 4,963,800 cells with 14,727,751 faces.

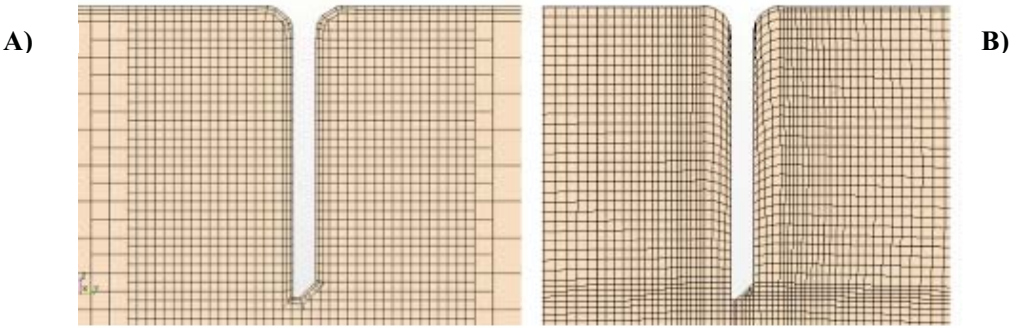

Figure 5: Unstructured (A) and block-unstructured (B) computational meshes showing the orifice region

A block-structured mesh was also used to compare the effect of meshing quality on the solution. The mesh was generated with ANSYS ICEM-HEXA at EDF R&D in Chatou, and has 3,203,058 cells, 9,572,485 faces. The cross-sections of the orifice region of both the block-structured and unstructured meshes are shown in **Figure 5**.

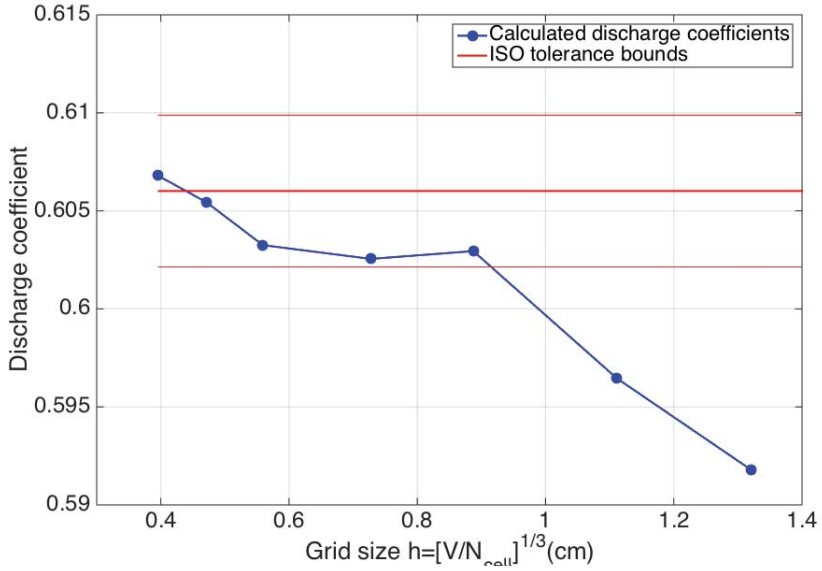

Figure 6: Grid convergence study for the unstructured mesh

The results of grid convergence study performed on the unstructured mesh are given in Figure 6. The finest grid size in is 0.4 cm. The grid sizes were chosen so as to approximately preserve the increment ratio of 1.2 so that 0.49cm, 0.6cm, 0.72cm, 0.9cm, 1.1cm and 1.35cm are the following sizes.

4.1.2 Benchmarking of RANS results

Results of all RANS simulations performed on the experimental geometry shown in Figure 2 are given in Figure 7. The figure includes the simulation results using both unstructured and block-structured meshes using linear k- ε model, and results of linear and cubic k- ε models for the unstructured mesh. The main observation is that all RANS results are approximately within 1% from both the experimental and ISO prescribed values for C. The sensitivity to two different mesh structures was found to be small as indicated by linear k- ε model results using two different meshes. Using the same unstructured mesh, cubic k- ε model was found to be the closer to the experimental result than the linear k- ε model. It is important to note that the ISO standard is not the benchmark in the experimental geometry since upstream piping geometry does not satisfy the requirements of the standard. Instead, the experimental result should serve as the benchmark for computation.

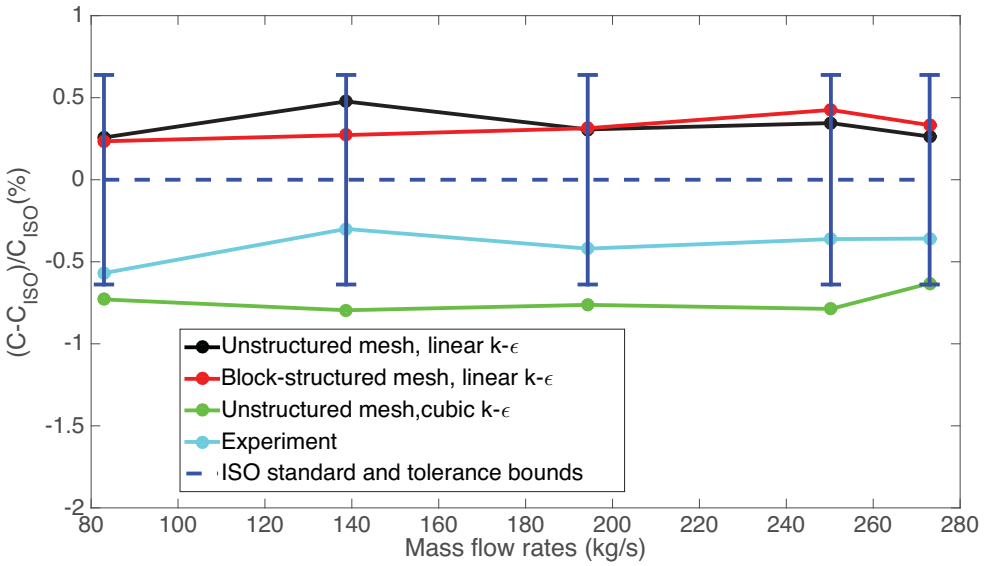

Figure 7: Summary of unsteady RANS simulation results benchmarked against ISO standard

4.1.3 Using RANS simulation to quantify spatial representativeness uncertainty

Spatial representativeness or spatial variability arises from treating a quantity as uniform and making measurement based on that assumption. The reasons for such simplified treatment of a physical process may be due to insufficient understanding of physical process or lack of model's accuracy.

Results of CFD simulation are post processed in order to see the dependence of CFD calculated discharge coefficient as a function of angular location θ of the pressure taps. The results are given in **Figure 8** for a flow rate corresponding to $\mathrm{Re}=3.7\cdot10^{5}$ using the block-structured mesh. The result indicates persistent

structure in the CFD calculated C coefficient as a function of angular tap location as a consequence of the geometry of the experimental circuit given in Figure 2. Results from the simulations at the other flow rates also exhibit similar structure in the calculated C coefficient.

Although the upstream flow development length in the experimental test meets the requirements of the ISO standard, our RANS simulation shows significant heterogeneity to the pressure field as a function of angular location of pressure taps used. An additional test is proposed with multiple pressure taps around the pipe in order to isolate this effect.

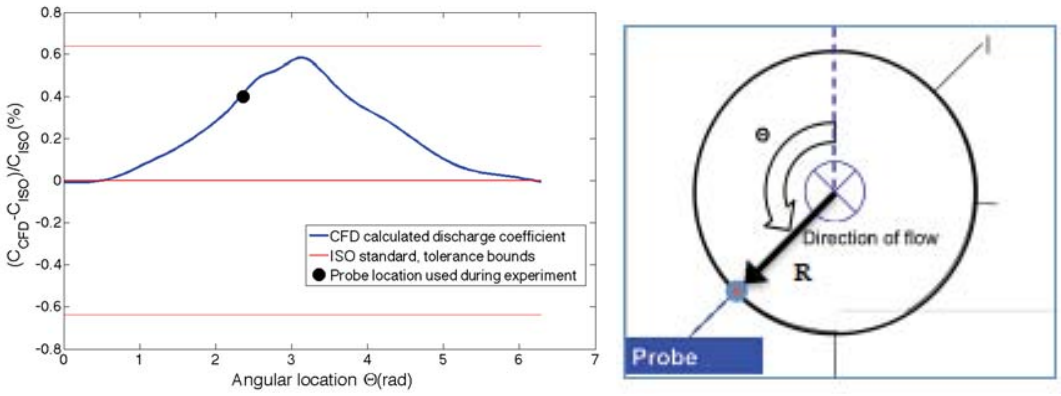

Figure 8: Dependence of CFD calculated discharge coefficient on angular location of pressure taps

4.2 Large Eddy Simulation

The specific pressure tapping configuration used in flow rate test measurement is called "D and D/2" pressure tap configuration meaning that pressure measurement is taken upstream at distance D from the orifice and D/2 downstream from the orifice. The β ratio of the test geometry is $\beta = 0.721$. We replicate the exact geometry in LES to be able to compare it with the test measurements.

4.2.1 LES mesh generation

In order to create the computational mesh for LES, we need to know the turbulent eddy sizes in all regions of the computational domain. Therefore, a preparatory RANS simulation was first performed to determine the turbulence eddy sizes, and LES mesh was constructed based on it. Figure 9 shows the integral turbulent length scale calculated as in equation (2)

$$L_{11} = C_{\mu}^{0.75} \frac{k^{1.5}}{\varepsilon} \tag{2}$$

In this equation k and ε are turbulent kinetic energy and dissipation rates respectively and $C_{\mu} = 0.09$. The turbulent integral length-scale calculated by Equation (2) gives a quantitative estimate of the size of turbulent eddies and enables the construction of the mesh for LES.

In creating the LES mesh, the $L_{11}/\Delta > 1$ criterion is used as the guideline in mesh generation and prism size of adjacent cells was minimized. Extensive work in the literature has shown the criterion used is sufficient to resolve up to the Taylor microscale[6]. Total size of the LES mesh was 17,166,922 cells, and number of prism layers 3 with constant thickness 4.75mm. Normal extruder with custom growth rate was used to create cells further away from the orifice. The LES mesh generated is shown in Figure 10, which

zooms into the orifice region and shows the extrusion length. The mesh generation is symmetric with respect to the orifice. The base size mesh is used in 2D both upstream and downstream the orifice and extruded additionally for 3D length.

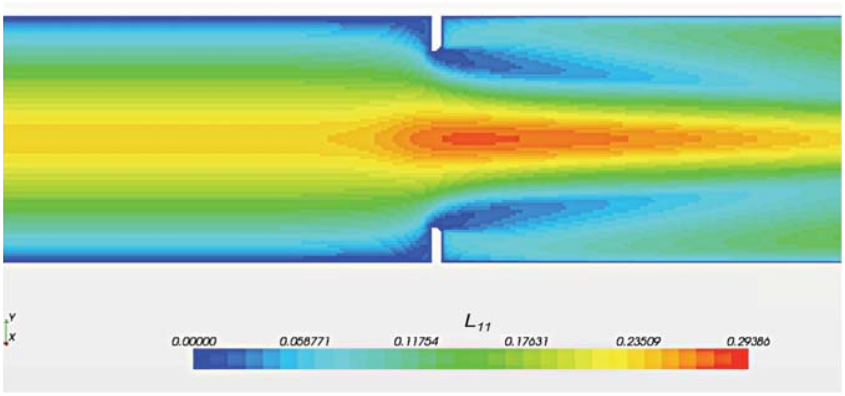

Figure 9:RANS simulation result of integral turbulent length scale given by equation (2) for the orifice plate test geometry at 100% power level

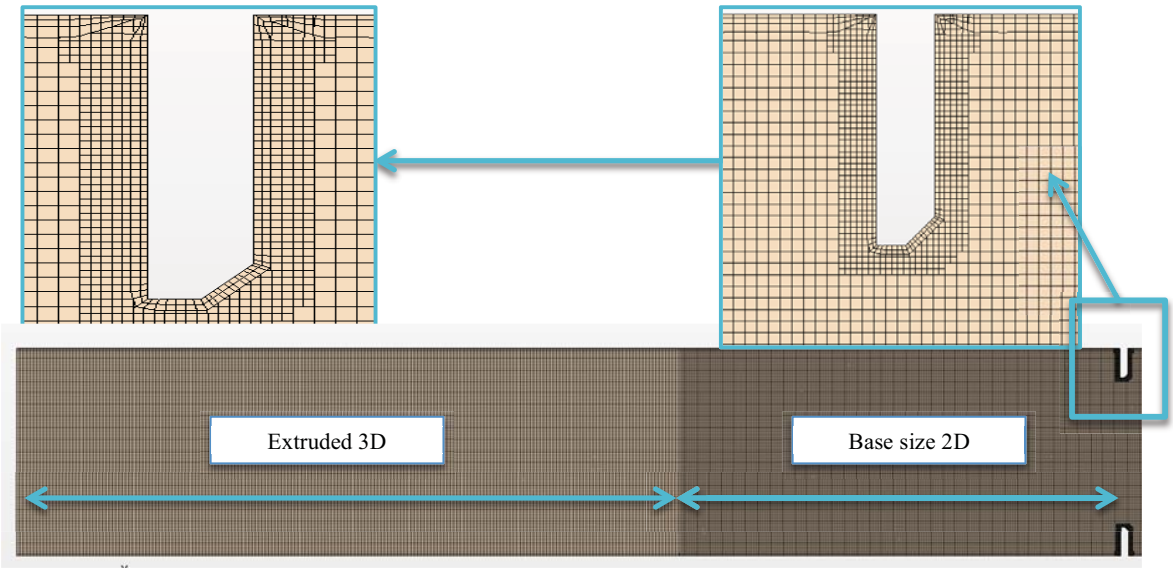

Figure 10: LES mesh. The base size mesh is used in 2D both upstream and downstream the orifice and extruded additionally for 3D length.

4.2.2 Boundary Conditions of LES

A fully developed flow profile is imposed as Inlet boundary condition in our LES simulations, while adopting the Synthetic Eddy Method (SEM) for generating sustained turbulence. SEM is demonstrated to produce a realistic turbulent inflow condition while preserving time, and length scale and coherent structure of turbulence[7]. A representative instantaneous velocity magnitude plot at the inlet is given in Figure 11.

Table 1: Physics models activated in LES

Models activated	Description
WALE sub-grid scale model	Computational inexpensive algebraic model for sub-grid scale stresses.
Second Order Implicit unsteady (3-time level)	Δt specified keeping Convective Courant number ~1.0
Synthetic Eddy Method	In order to generate sustained turbulence at the inlet boundary

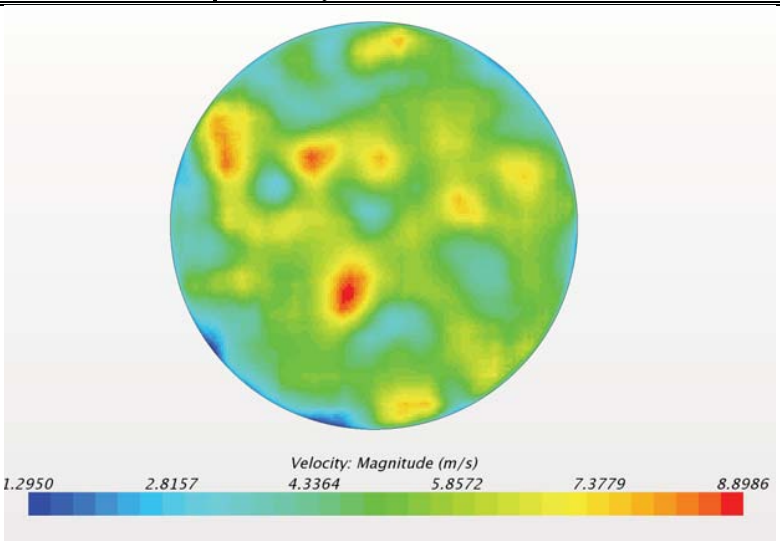

Figure 11: Inlet velocity magnitude plot for LES. Fully developed flow profile and Synthetic Eddy Method is used to generate the required mass flow rate and sustained turbulence respectively.

The modeling of subgrid scales is based on the wall-adapting local eddy-viscosity (WALE) model, leveraging its generality and extensive assessment[4]. In this work near wall modeled (NWM) LES was adopted in order to keep the computational cost low (practicable) in a high Reynolds number case such as this. Validity of using near wall modeled LES is discussed by Baglietto et al[4].

4.2.3 Results of the LES simulation

Figure 12 and Figure 13 shows velocity magnitude and pressure fields as resolved by LES. The origin of the origin of the fluctuation of pressure differential signals observed during the test as described in Section 3.2 can be explained from the presence of coherent structures, visible in the alternating high and low pressure vortices originating at the orifice edge in the LES resolved pressure plot in Figure 13. Other hypothesis behind the phenomenon need to be tested, but not included in this publication.

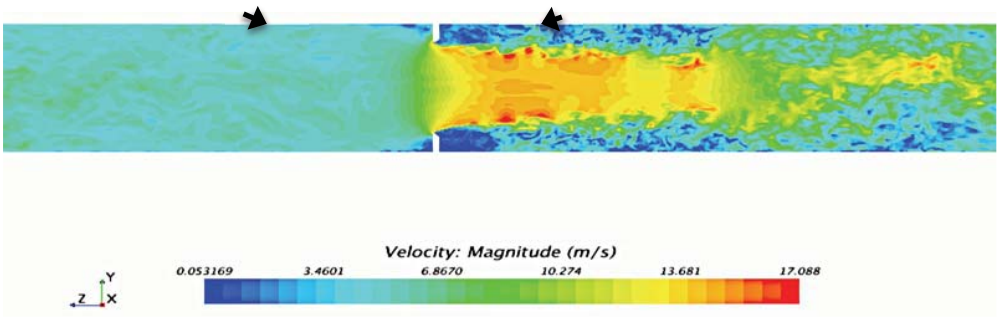

Figure 12: LES calculated velocity magnitude field. Black arrows show the locations of upstream downstream pressure taps

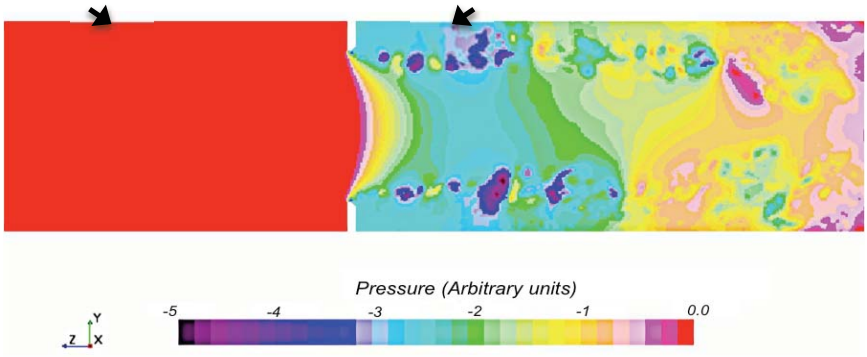

Figure 13: LES result of pressure field at 100% power. Black arrows show the locations of upstream downstream pressure taps

4.2.4 Benchmarking LES results using the ISO standard

In order to validate LES results, the discharge coefficient C described in section 2 calculated by LES is benchmarked against the discharge coefficient prescribed by the ISO standard. Figure 14 shows the LES calculated discharge coefficient for 10 sec simulations for 100%, and 80% power levels respectively. For all power levels, the time average of the LES calculated C coefficient C_{LES} given in Equation (3) is within 0.1% of the value prescribed by the ISO standard. The difference between the ISO standard result and the LES simulation result is a systematic error which is defined as the representativeness.

The discharge coefficient is calculated in LES as given in equation (3). The upstream and downstream pressure values are taken from point pressure probes as shown in Figure 12. At each time instant, both upstream and downstream pressures are probed and the C coefficient is calculated as a function of simulation time. When comparing with the values from the standard, time average value of LES, the calculated C coefficient is used.

$$C_{LES}(t) = q_m \frac{4}{\pi} \sqrt{1-\beta^4} \frac{1}{d^2 \sqrt{2\rho(p_{upstream}(t) - p_{downstream}(t))}} \tag{3}$$

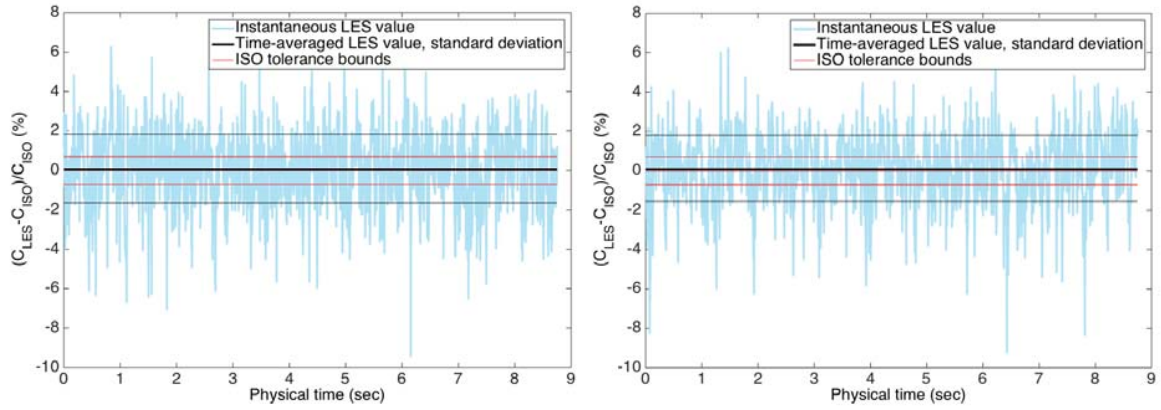

Figure 14: Discharge coefficient C calculated from LES at A) 100%, B) 80% power levels. The time averaged LES results were shown to reproduce ISO prescribed values of C within 0.1%.

4.2.5 Spectral analysis using LES results

A spectral analysis was carried out on both the test signal and LES result in order to characterize the temporal representativeness uncertainty of the measurement. Test data of duration 1200 seconds with sampling frequency of 1000Hz is given in section 3.2. On the other hand, LES is of a ~10 sec physical time and a time step of 2.5e-4 sec (equivalent of 4000Hz sampling rate). Therefore, the lowest frequency components of test signal (~0.001 sec) are not accessible by LES due to limited computational resources. The results of the analysis using power spectral density are given in Figure 15.

Power Spectral Density (PSD) is used in order to assess the distribution of the power of a time varying signal as a function of frequency[8]. PSD is defined as

$$P_{xx}(f) = \int_{t=0}^{T} e^{2\pi i f t} R_{xx}(t)\, dt \tag{4}$$

where the time-averaged auto-correlation of the sequence is defined as $R_{xx}(t) = \frac{1}{T-t}\int_{t=0}^{T} p(\tau)p(t+\tau)d\tau$ [1]

for a time dependent pressure signal $p(t)$ of length T. The PSD (units Pa^2/s) is then non-dimensionalized using

$$\Phi_p(f) = \frac{P_{xx}(f)}{4q^2 d/V} \tag{5}$$

where $q = \rho V^2/2$ is the dynamic pressure in the pipe. V is taken to be cross section averaged velocity of the fluid in the pipe. In this paper, the PSDs for the raw test data, is calculated using a built-in power spectral density function in MATLAB, and the result is given in Figure 15. Peaks at frequencies 50Hz(2n+1), n=0,1,2… are indicative of a measurement related noise. In comparing with the simulation, the measurement noise can be smoothed out using moving average method.

Figure 15 shows the LES spectrum along with raw test data spectrum. The sharp drop in spectrum of the LES results at 3Hz is an artifact of the algorithm used to construct PSD. The order of magnitude, and

[1] 6.011 course note, Spring 2010, ocw.mit.edu

shift in spectrum with flow rate are reproduced using LES. However, close examination of the shape of the spectrum reveals significant differences. While the exact reasons are not understood currently, factors contributing to the shape of the spectrum might be the simulated and test signal-sampling frequencies and the lengths of signals. Test signal is of sampling frequency 1000Hz (data acquisition time of 1200sec) whereas LES simulation as done with a time step equivalent of 4000Hz (simulation time of 10sec) sampling frequency. The Courant number of the simulation dictated the time step in LES. More detailed data on pressure measurement configuration will be needed to understand potential damping of test pressure signals from the pressure taps.

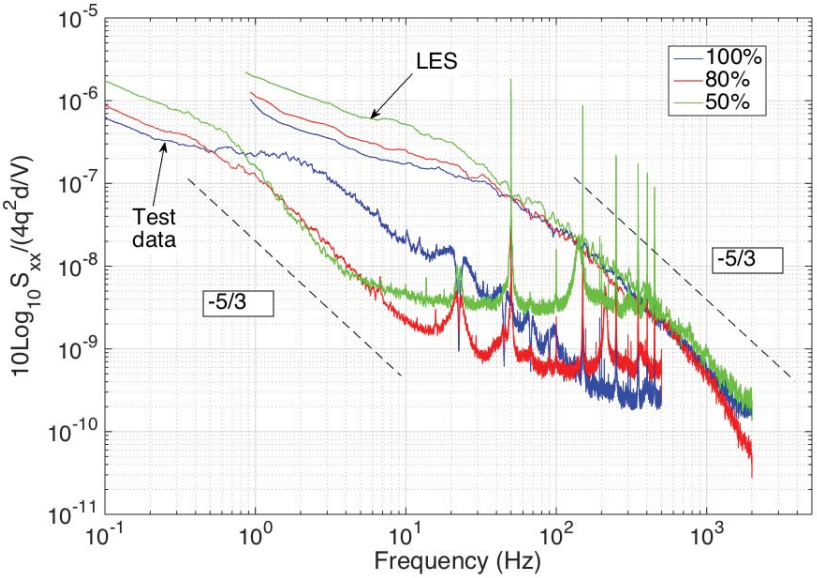

Figure 15 PSD of test (section 3.2) and LES simulated pressure drop data. Test signal is the raw signal with no filtering. Vertical axis is non-dimensionalized using equation (5) for comparison

Impulse line or gauge line is the tubing or piping which connect the pressure taps on the primary element (orifice pipe) to a secondary element (recording device or transmitter)[9]. The general guideline provided by Harris and McNaught[10] lists factors that could induce potential pulsation in pressure measurement. These are: impulse line diameter and length, location of secondary device, location of pressure tapping, ambient temperature, temperature fluctuation, fluid type, valves, connections for venting. Although we do not have access to detailed configuration of the impulse line at the plant where the test is taken, photographs taken suggest that impulse lines are long with multiple bends and turns. This could explain deviation in frequency spectrums produced by LES and measured spectrum from the test.

5 CONCLUSIONS AND FUTURE WORK

Partial results of the development of methodology for characterizing representativeness uncertainty in performance indicator measurements in power plant are presented in this work. The specific performance indicator considered is steam generator mass flow rate measurement by means of the orifice plate. It is an important performance indicator contributing to a large portion of total uncertainty in the calculation of nominal thermal power at 100%.

RANS simulations were implemented using STAR-CCM+ to identify and characterize the spatial representativeness error in mass flow rate measurement using an orifice plate in non-straight pipe geometry. RANS was shown to distinguish sub 1% trends in the extent of the dependence of the mass

flow rate measurement result to the angular location of pressure taps used. These RANS results were then used to identify and quantify the spatial representativeness in this measurement.

Next, LES calculations were performed to better capture the complex flow structures generated by the orifice edge and their effects. The time averaged LES results were found to be within 0.1% of the value prescribed by the ISO standard in a benchmark comparison. The results of LES were then used to identify and qualitatively determine frequency spectra of chaotic pressure differential signals, and were compared to the observed test data. The order of magnitude, and shift in spectrum with flow rate from the test data are reproduced using LES. However, the exact comparison of the shapes of the spectrums from both the simulation and test data is not possible due to the configuration of impulse line at the measurement setting which is known to alter the shape of the frequency spectrum.

We demonstrated in this work that CFD tools can be applied in mass flow measurement setting using an orifice plate with significant confidence as demonstrated by both RANS and LES results. CFD simulations are also shown to provide qualitative and quantitative insight into potential representativeness problems that can occur when adopting measurement standards in non-straight piping geometries.

This work is part of a wider ongoing Ph.D work on representativeness uncertainty in measurements of performance indicators at nuclear plants. A full methodology on characterizing, assessing spatial, temporal and modeling uncertainties will be developed based on several future case studies the first of which is the current work.

6 ACKNOWLEDGMENTS

This work was supported by funding from EDF R&D and benefited greatly from the suggestions of Yvan Caffari the EDF designated technical manager of this project. The structured mesh used in RANS simulation was provided by EDF R&D at Chatou.

7 REFERENCES

1. *Application of Orifice Plates for Measurement of Feedwater Flow: EdF Plant Experience*. 2001, EPRI: Palo Alto, CA.
2. ISO, *Measurement of fluid flow by means of pressure differential devices inserted in circular cross-section conduits running full - Part 2: Orifice plates*. 2003.
3. William.L. Oberkampf, C.R., *Verification and Validation in Scientific computing, Cambridge University Press*, ed. C.U. Press. 2010.
4. Baglietto, E. and H. Ninokata, *Anisotropic eddy viscosity modeling for application to industrial engineering internal flows.* International Journal of Transport Phenomena, 2006. **8**(2): p. 109.
5. VEAU, J. and J.-G. GUILLET, *Internal EDF report*. 2012, EDF R&D.
6. Jayaraju, S.T., E.M.J. Komen, and E. Baglietto, *Suitability of wall-functions in large eddy simulation for thermal fatigue in a T-junction.* Nuclear Engineering and Design, 2010. **240**(10): p. 2544-2554.
7. Jarrin, N., et al., *A synthetic-eddy method for generating inflow conditions for large-eddy simulations.* International Journal Heat Fluid Flow 2006. **27**(4): p. 585–593.
8. Qing, M. and Z. Jinghui, *Orifice-induced Wall Pressure Fluctuations and PipeVibrations.* Theory and Modeling of Fluid Excitations, 2007. **79**: p. 25-40.
9. Donald, S., et al., *Pulsation effects on orifice meters, Operations conference*, in *Operations conference*. 2002, American gas association: Chicago, Illinois.
10. Reader-Harris, M.J. and J.M. McNaught, *Best practice guide, Impulse lines for differential pressure flowmeters*, NEL, Editor. 2005.